# Orthogonal Molecular Structure for Better Host Material in Blue Phosphorescence and Larger OLED White Lighting Panel

*Lei Ding, Shou-Cheng Dong, Zuo-Quan Jiang,* Hua Chen, and Liang-Sheng Liao**

**High-efficiency blue phosphorescence devices with external quantum efficiencies above 25% are developed using a new bipolar host material, diphenyl(10-phenyl-10*H*-spiro[acridine-9,9′-fluoren]-2′-yl)phosphine oxide (POSTF), which is constructed in orthogonal molecular structure with a spiro-coree. The separation of bipolarity from effective spiro-fluorene-triphenylamine (STF) structure is elucidated and its versatility in device is evaluated by two kinds of sky-blue phosphors. Noticeably, large-size white light-emitting panel (150 mm × 150 mm) is fabricated with max power efficiency of 75.9 l m W$^{-1}$ using this new host.**

## 1. Introduction

In recent years, phosphorescent organic light-emitting diodes (PHOLEDs) have drawn tremendous attention for the PHOLEDs can achieve theoretical 100% internal quantum efficiency that is much higher than fluorescent organic light-emitting diodes.[1] Up to now, the PHOLEDs have made great progress in high efficiency and the progress is along with the development of triplet host materials, especially after the advent of bipolar host materials.[2] Among these bipolar host materials, the blue host requires a compromise between the bipolar transporting property and relatively larger band gap of the material. Meanwhile, efficient exciton confinement by keeping a higher triplet energy level of blue host material than that of the emissive guest molecules is also necessary, thus, this requirement is sometimes difficult to fulfill.[3] Although it is not easy, numerous blue bipolar host materials were designed and prepared, with which the blue phosphorescent performances can reach high external quantum efficiency (EQE) of ≈20%, power efficiency (EQE) of ≈40 lm W$^{-1}$ and show low efficiency roll-off at brightness of 1000 cd m$^{-2}$.[4] However, the better host materials that can fabricate blue devices with EQE > 25%, power efficiency (PE) >50 lm W$^{-1}$ and low efficiency roll-off at 5000 cd m$^{-2}$ are still rare.[5] Considering the pursuit of various blue emitters is still ongoing,[6] it is also necessary to develop new host materials to test different kinds of emitting phosphors. Furthermore, another main application for blue hosts is for the high-efficiency white light emission; their performances on large-size lighting panels are fascinating but still a blank in recent literature reports.[6] Therefore, constant efforts should be devoted to developing good host materials that can achieve high efficiency and flat efficiency roll-off simultaneously in blue/white PHOLEDs.

The compounds with spiro-core are good candidates in constructing bipolar materials for the inherent orthogonal structure of two molecular halves. In addition, this approach can also efficiently suppress intermolecular interaction by their adamant backbone, resulting in better solubility and cause entanglement in the amorphous state, then hinder recrystallization.[7] The development of spiro host material, however, is relatively slower as compared with other series of host materials. In 2005, the first example of spiro host materials named SSS based on 9,9′-spirobifluorene core is reported, which obtained EQE of ≈10% for red phosphorescence.[8] In 2008, the first spiro bipolar molecule D2ACN integrated with electron-rich diphenylamine and electron-deficient nitrile is prepared, but the EQE is just slightly improved to 10.8% with PE of 13 lm W$^{-1}$ as red host material.[9] To date, there are just several attempts on blue hosts based on spiro-structure and the device performances are moderate.[10] Recently, we reported a blue host material SSTF based on new STF core, which could achieved a PE of 41.5 lm W$^{-1}$ and an EQE of 18.7%.[11] In the STF molecular structure, a triphenylamine moiety is placed in vertical configuration to fluorene. This configuration endows good hole-transporting ability to STF and makes it unnecessary to introduce any other arylamine groups on spiro backbone that always reduces the triplet energy (such as D2ACN). On the other hand, the fluorene moiety can be further modified by appending electron-deficient groups to enhance bipolar property. Herein, we design and prepare a new spiro host material POSTF by appending phosphine oxide group on the fluorene moiety. It demonstrates very high EQE and extremely low efficiency roll-offs for sky-blue (small size) and white (large size) phosphorescent devices.

L. Ding, Dr. S.-C. Dong, Dr. Z.-Q. Jiang, Dr. H. Chen, Prof. L.-S. Liao
Jiangsu Key Laboratory for Carbon-Based Functional Materials & Devices
Institute of Functional Nano & Soft Materials (FUNSOM)
Soochow University
Suzhou, Jiangsu 215123, P.R. China
E-mail: zqjiang@suda.edu.cn; lsliao@suda.edu.cn

**DOI: 10.1002/adfm.201403402**

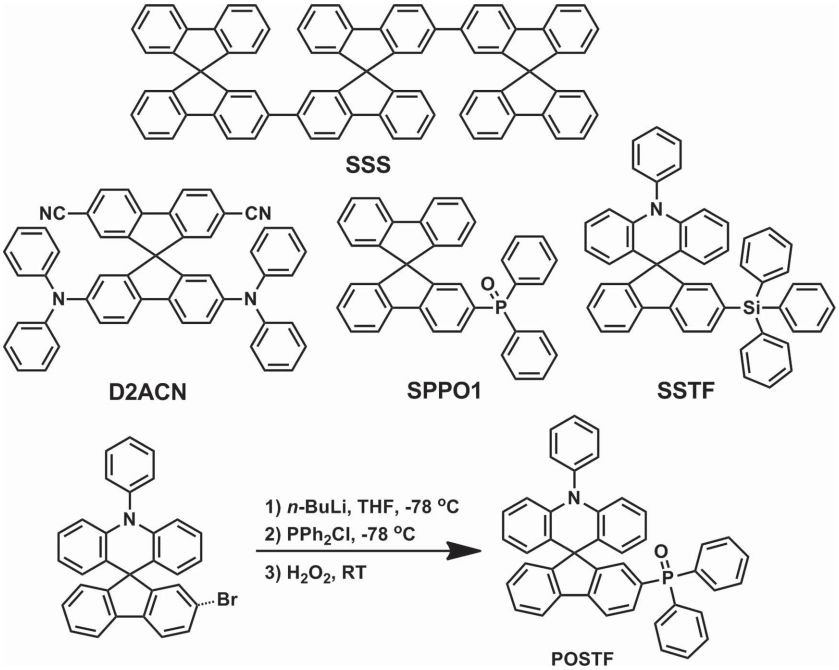


**Scheme 1.** The spiro host materials and the synthesis of new host material.

## 2. Results and Discussion

The synthesis of POSTF is straightforward (**Scheme 1**). The central triphenylamine annulated fluorene is synthesized by 2-bromo triphenylamine and 2-bromo-fluorenone as reactants.[12] Then the brominated spiro-structure was treated with n-BuLi, coupled with chlorodiphenylphosphine, and oxidized with hydrogen peroxide to afford the final product POSTF. All the compounds were characterized by $^{1}$H NMR, $^{13}$C NMR, EI-MS and element analysis. Thermogravimetric analysis and Differential scanning calorimetry (DSC) techniques were utilized to investigate its thermal stability. Benefitted from the rigid spiro STF backbone, the compact molecule POSTF exhibited both high decomposition temperature (356 °C) and high glass transition temperature (119 °C). We also notice these data are higher than those of SPPO1 (Scheme 1),[13] the spirobifluorene analogue of POSTF, indicating the introduction of triphenylamine not only will possibly improve hole injection, but also can enhance their thermal stability.

The absorption and photoluminescence spectra of POSTF were tested in dilute toluene solutions and the phosphorescent spectrum was obtained at 77 K in 2-methy-THF matrix. The normalized spectra are depicted in **Figure 1**. Absorption spectrum in vacuum deposited thin film was also tested and its optical bandgap in solid state was determined as 3.45 eV from the onset wavelength. The phosphorescence spectrum was measured in 2-methyl-THF solution at 77 K, and the triplet energy of POSTF was determined as 2.80 eV.

The oxidation cyclic voltammetry (CV) curve of POSTF was obtained in DCM solution. As shown in Figure S3 (Supporting Information), reversible oxidation process was observed corresponding to the oxidation/reduction of spiroarylamine. No obvious reduction process was found in DMF solution. From the CV data and optical bandgap (3.63 eV) in DCM solution, the highest occupied molecular orbital (HOMO) and lowest unoccupied molecular orbital (LUMO) of POSTF in solution can be calculated as 5.34 eV and 1.71 eV, respectively. Considering that the other materials in the OLED normally use the energy level data obtained from thin films, instead of from solutions, the HOMO level of POSTF was collected in solid state by ultraviolet photoelectron spectroscopy, and then the LUMO was calculated using the obtained HOMO and the optical bandgap in deposited thin film. As a result, the HOMO/LUMO were determined as 5.57/2.12 eV, respectively. The HOMO and LUMO distribution of POSTF was also investigated by density functional theory (DFT) calculations at the B3LYP/6–31 g(d) level. The optimized structure of POSTF shows the triphenylamine leans toward the PO group, suggesting a possible space electrostatic attraction between the donor and acceptor (**Figure 2**).

As expected, the HOMO and LUMO of POSTF are separately distributed on each side of the spiro backbone. The HOMO mainly locates on the electron donating triphenylamine. And like other spirobifluorene analogues, the LUMO is dispersed over the fluorene unit with minor extension to the adjacent P═O group due to the unconjugated linkage. The separated HOMO and LUMO suggest its bipolar property with separated hole and electron transporting channels.

This HOMO/LUMO separation can also be achieved by conjugation interruption using $sp^3$ atom (carbon or silicon) in which the donor and acceptor groups are placed at different sides of molecule.[14] In a spiro system, the separation hub is also a $sp^3$ spiro-carbon, but the situation may be a bit uncertain. That is because a spiro-conjugation effect may exist in a spiro compound, which means two orbitals in different planes have the possibility to overlap their orbital integral. But there are symmetrical requirements. General speaking, two $\pi$-networks

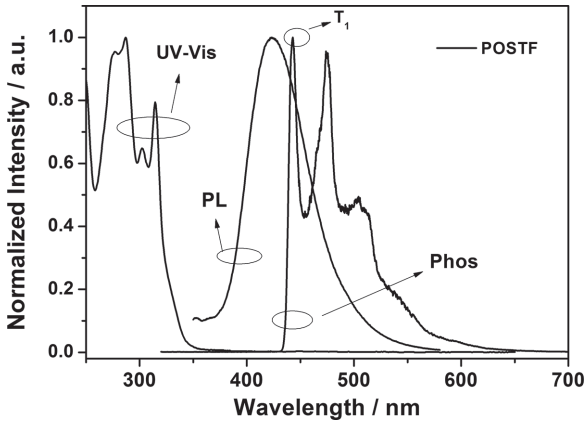


**Figure 1.** UV–Vis absorption, fluorescence (r. t) and phosphorescent (77 k) spectra of POSTF.

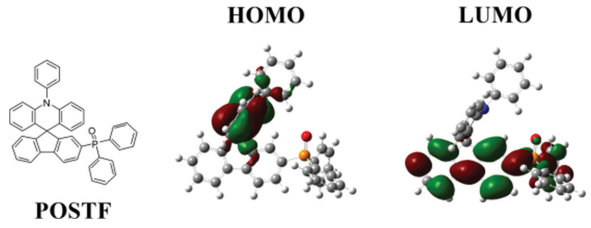


**Figure 2.** Frontier molecular orbitals (FMOs) distribution of POSTF (iso value = 0.02).

are joined by a spiro atom only the molecular orbitals of the two $\pi$-subsystems that have the same symmetry may interact, leading to molecular orbitals spanning the entire system. In other words, only those orbitals of the subsystems that are antisymmetric with respect to the two planes lead to a nonzero overlap required for intramolecular interaction.[15] To address this question in our case, we dissect the STF into acridine and fluorene components, and their HOMO/LUMO contours are showed in **Figure 3**. Compared with the contour in Figure 2, it is easy to find that the frontier orbitals of POSTF are combined by the HOMO of acridine and the LUMO of fluorene, both of them are symmetric orbitals. Therefore, the HOMO/LUMO distributions in STF system should have little interaction to each other.

Since, the POSTF had high triplet energy for blue phosphorescent emitters, possessed both electron-/hole-transporting moieties and exhibited suitable HOMO/LUMO levels for charge injection, it can be used as host materials in blue phosphorescent devices to evaluate its performances. Blue PHOLEDs based on commonly used sky-blue iridium complex iridium(III) bis(4,6-(difluorophenyl)-pyridinato-N,C′)picolinate (FIrpic) were fabricated. And recently, another kind of iridium emitters without fluorine atom on the complexes has been proposed.[6d,g] Thus, we also used this new type of sky-blue emitter named *fac*-tris[(2,6-diisopropylphenyl)-2-phenyl-1H′-imidazo[e]]iridium(III) *fac*-Ir(iprpmi)$_3$ to assess POSTF as blue host, using device structure of ITO/1,4,5,8,9,11-hexaazatriphenylene-hexacarbonitrile (HAT–CN) (10 nm)/1,1-bis[4-[*N*,*N*-di(p-tolyl)amino]phenyl]cyclohexane (TAPC) (45 nm)/POSTF: dopant (X vol%, 20 nm)/TmPyPB (40 nm)/Liq (2 nm)/Al (100 nm). HAT–CN was used as hole injecting material. TAPC, which has a high ET and carrier mobility serve as hole-transporting layer (HTL) and electron-blocking layer. TmPyPB and Liq were used to form electron-transporting layer

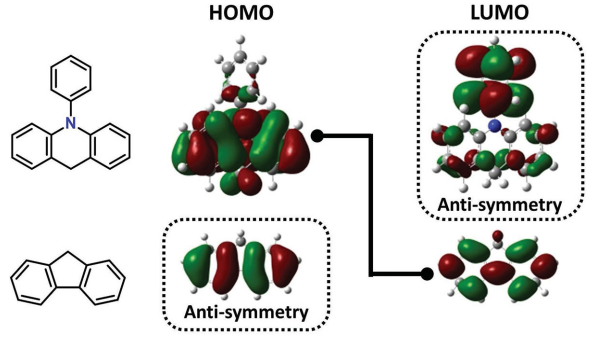


**Figure 3.** Analysis of frontier orbital symmetry for possible spiro-conjugation.

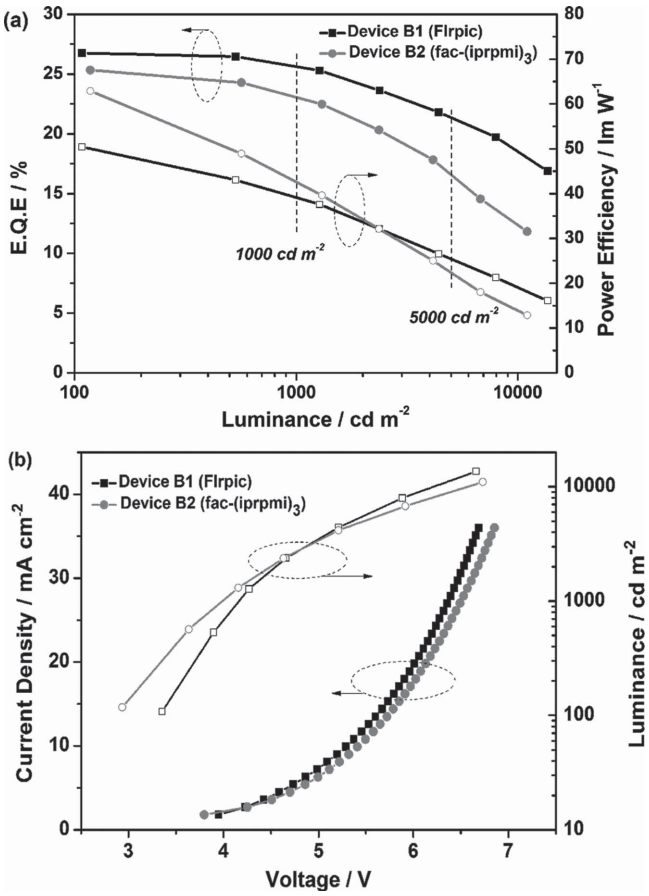


**Figure 4.** EQE and power efficiency versus luminance a), current density and luminance versus voltage b) of device B1 and B2.

and electron-injecting layer. Dopants for Device B1 and B2 are FIrpic (15 vol%) and *fac*-Ir(iprpmi)$_3$ (12 vol%), respectively. As expected, these two devices show excellent performances. **Figure 4**a depicts the EQE and PE as a function of luminance. Figure 4b illustrates the electroluminescent (EL) characteristics of the sky-blue phosphorescent devices. The detailed electroluminescence data are summarized in **Table 1**. The maximum EQE and PE of Device B1 (FIrpic) are 26.8% and 50.5 lm W$^{-1}$ with the Commission International de I'Eclairage (CIE) coordinates

**Table 1.** Summary of electroluminescence data for PHOLEDs.

| Device[a)] | V [V][b)] | CE [cd A$^{-1}$][c)] | PE [lm W$^{-1}$][c)] | EQE [%][c)] |
|---|---|---|---|---|
| B1 | 4.1 | 53.9, 51.9, 43.3 | 50.5, 39.5, 25.7 | 26.8, 25.6, 21.5 |
| B2 | 3.9 | 58.8, 54.1, 39.2 | 62.9, 42.7, 22.3 | 25.3, 23.1, 16.7 |
| W1 | 4.5 | 53.2, 52.4, 43.7 | 44.4, 36.7, 23.4 | 24.6, 24.1, 20.4 |
| W2 | 4.3 | 75.7, 68.8, 51.0 | 64.9, 49.6, 29.2 | 27.2, 24.8, 18.5 |
| W3 | 25.7 | 66.7, 62.0, — | 63.9, 38.6, — | 21.9, 20.3, — |
| W4 | 25.5 | 98.4, 118.2, — | 75.9, 71.5, — | 41.8, 39.7, — |

[a)]Blue device (B1 & B2) and white device (W1 & W2) size: 0.03 cm$^2$. Large-size white device (W3 without diffuser film & W4 with diffuser film) size: 150 ×150 mm$^2$; [b)]Driving voltage at 1000 cd m$^{-2}$; [c)]Efficiencies in the order of maximum, at 1000 cd m$^{-2}$ and at 5000 cd m$^{-2}$.

of (0.14, 0.33). These results are among the best results of FIrpic-based devices. Moreover, Device B1 also shows very flat EQE roll-off: at 1000 cd $m^{-2}$, the EQE is only slightly reduced to 25.6%. Even at high brightness of 5000 cd $m^{-2}$, the EQE is still as high as 21.5%. This result is much better than that of previous spiro-host SSTF, indicating the bipolar design in spiro-molecule is can make dramatically improvement in device performance. As compared with Device B1, the Device B2 exhibited much lower driving voltage of 2.8 V at 100 cd $m^{-2}$ and higher PE of 62.9 lm $W^{-1}$. Due to the more greenish EL spectrum of *fac*-Ir(iprpmi)$_3$, the EQE of B2 is 25.3%, slightly lower than B1. B2 also exhibits relatively large efficiency roll-off than B1, especially at high brightness. Unlike FIrpic, *fac*-Ir(iprpmi)$_3$ has very shallow HOMO of 4.8 eV, much higher than the host and the HTL. This makes it act as strong hole trapping sites in the emitting layer (EML). At low current, the high lying HOMO of *fac*-Ir(iprpmi)$_3$ may facilitate hole injection, resulting in low driving voltage. As the current increases, injected holes will be slowed down by *fac*-Ir(iprpmi)$_3$ and considerable proportion of holes may be trapped on the dopant, accumulating holes in the EML. According to the energy diagram, holes will be the predominating charge carriers in the EML despite the bipolar property of the host. The hole-trapping *fac*-Ir(iprpmi)$_3$ deteriorate the situation of unbalanced charge carriers in the EML. The excessive holes and the direct combination of electron and hole on the dopant may be the reason of B2's large efficiency roll-off at high brightness. On the other hand, FIrpic in B1, which has a relatively low lying LUMO, may compensate the unbalanced charge carriers by increasing electron injection into the EML at high current. As a result, B1 shows a bit better roll-off than B2 at 5000 cd $m^{-2}$. In general, both results exceeding 25% EQE proved the superiority and versatility of POSTF as efficient blue host.

The good performance of both PHOLEDs qualified POSTF as potential host materials for white PHOLEDs, and furthermore, it is very fascinating to use this host in large-area lighting panel. That means we would enlarge the active luminescent size from 3 mm × 3 mm to 150 mm × 150 mm. It is not only a test for host capability but also a test for material's uniformity. Prior to this study, two types of small-size WOLED were investigated to optimize the device structure for large-size panel. The first device (W1) is a three color-based PHOLED with one sky-blue EML and one green and red EML. This kind of configuration can realize balanced properties between efficiency and color quality. The other device (W2) features only one EML containing sky-blue and yellow phosphorescent dopants. With single EML, the device can be simplified and achieve high efficiency (Figure S9, Supporting Information). The results of W1 and W2 are summarized in Table 1. Both W1 and W2 achieve EQE greater than 24%. The maximum EQE of W2 reaches 27.2%.

Considering the simple structure and high efficiency of W2, we choose its structure to construct large area devices. The lighting panel we fabricated had a size of 190 mm × 177 mm with 150 mm × 150 mm active area. The device structure of the panel is ITO/HAT–CN (10 nm)/TAPC (45 nm)/POSTF: 15 vol% FIrpic: 1 vol% PO-01 (20 nm)/ TmPyPB (40 nm)/ Liq (2 nm)/Al, in which the concentration of orange dopant iridium(III) bis(4-phenylthieno[3,2-c] pyridinato-N,C2′) acetylacetonate (PO-01) should be lower than that of FIrpic in order to obtain a white emission. Besides that, in view of existing

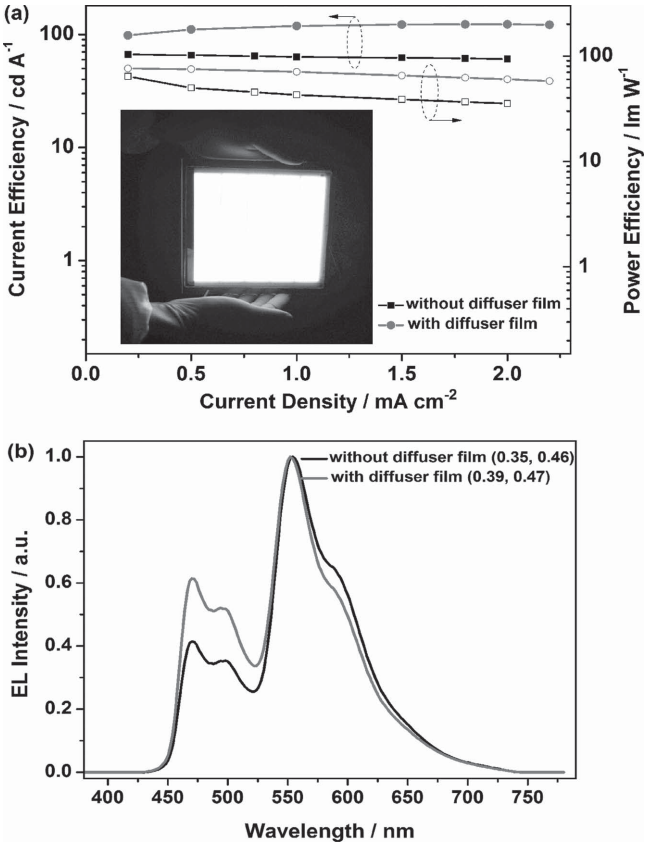


**Figure 5.** a) Current efficiency–current density–power efficiency characteristics, with devices measured in forward direction with and without outcoupling enhancement techniques. The inset shows the image of the large-area OLED lighting panel. b) The corresponding normalized EL spectra.

problem (such as IR-drop, uniformity, or local heating) of large-size OLEDs lighting panel at the present stage, we adopted the method of series connection of devices which can reduces power loss due to series resistance. Encouragingly, excellent quality white OLED panel is obtained using this device structure. As shown in **Figure 5**a, the device (W3) without diffusers shows the maximum efficiencies of 66.6 cd $A^{-1}$ for CE, 63.8 lm $W^{-1}$ for PE and 21.9% for EQE. Furthermore, by applying state of the art light out-coupling film (Kimoto), the efficiency of the device can be boosted to 98.4 cd $A^{-1}$ for CE, 75.9 lm $W^{-1}$ for PE. The inset of Figure 5a shows the image of its working state of high performance white OLED panel. The EL spectra of the large area OLED panel with and without diffuser are shown in Figure 5b.

The angular dependence of chromaticity and normalized EL intensity as a function of emission angle are depicted in Figures S12 and S13 (Supporting Information), respectively. A quite good spatial uniformity in chromaticity was realized by using POSTF host material.

## 3. Conclusion

A new spiro host material POSTF is synthesized, characterized and fully assessed in PHOLED devices with small size and

large size. With FIrpic as dopant, the device can achieve power efficiency of 50.5 lm $W^{-1}$, EQE of 26.8%, and also presented low roll-off at high brightness of 5000 cd $m^{-2}$. By using another sky-blue emitter *fac*-Ir(iprpmi)$_3$ with higher HOMO level, the POSTF showed its university and the corresponding EQE of device also exceeded 25%. Comprehensively considering these indexes, the performance of POSTF is a big leap compared with previous spiro host material, and it is catching up the step of other series top bipolar host material for both blue and white electrophosphorescent devices. It proved that a spiro-structure can be facilely modified in constructing high-triplet-energy bipolar host material with excellent performance if suitable spiro backbone is sorted out. Due to its spiro-bipolar property and natural chemical stability, we are encouraged to fabricate a large-size white lighting prototype device with active area of 150 mm × 150 mm. In this device, a PE of 63.9 lm $W^{-1}$ was achieved. By applying state-of-the-art out-coupling technique, this PE can be further improved as high as 75.9 lm $W^{-1}$. This is also the first report for bipolar host material used in large-size PHOLED panel.

## 4. Experimental Section

*Measurements and Characterization*: $^1$H NMR and $^{13}$C NMR spectra were obtained on a Bruker 400M spectrometer at room temperature. Mass spectra were performed on a Thermo ISQ mass spectrometer using direct exposure probe. Elemental analyses were performed using Vario EL III microanalyzer. FT-IR spectrum was obtained on a Bruker Optics VERTEX 70 FT-IR spectrometer at room temperature. UV–Vis absorption spectra were recorded on a Perkin Elmer Lambda 750 spectrophotometer. PL spectra and phosphorescent spectra were recorded on a Hitachi F-4600 fluorescence spectrophotometer. Differential scanning calorimetry was performed on a TA DSC 2010 unit at a heating rate of 10 °C $min^{-1}$ under nitrogen. The glass transition temperatures were determined from the second heating scan. Thermogravimetric analysis was performed on a TA SDT 2960 instrument at a heating rate of 10 °C $min^{-1}$ under nitrogen. Temperatures at 95% weight loss were used as decomposition temperatures. Cyclic voltammetry was carried out on a CHI600 voltammetric analyzer at room temperature with a conventional three-electrode configuration consisting of a platinum disk working electrode, a platinum wire auxiliary electrode, and an Ag wire pseudo-reference electrode with ferrocenium-ferrocene (Fc+/Fc)as the internal standard. Nitrogen-purged dichloromethane was used as solvent for oxidation scan and DMF for reduction scan with tetrabutylammonium hexafluorophosphate (0.1 M) as the supporting electrolyte. The cyclic voltammograms were obtained at scan rate of 100 mV $s^{-1}$. Ultraviolet photoelectron spectroscopy analysis were carried out with an unfiltered HeI (21.2 eV) gas discharge lamp and a hemispherical analyzer. DFT calculations were performed using B3LYP/6–31G(D) atomic basis set.

*Device Fabrication and Characterization*: Organic light-emitting diodes were fabricated on the cleaned glass substrates precoated with 110 nm ITO (15 Ω $\square^{-1}$) were cleaned with detergent, acetone, alcohol, distilled water, and then in an ultrasonic solvent bath. After baking in a heating chamber at 110 °C for 4 h. The ITO-glass substrates were treated with UV ozone for 15 min. All layers were deposited by thermal evaporation under a base vacuum around 10–6 Torr (1 Torr = 133.32 Pa). The organic materials and metal were evaporated in the rate of 3–5 Å $s^{-1}$ and 8–10 Å $s^{-1}$, respectively. The luminance, EL spectra and the CIE coordinates of all devices were measured by using a PR-670 photometer. Current density–voltage (*J*–*V*) measurements were carried out using a Keithley 2400 Source Meter. The emitting area of the white OLED devices and lighting panel are 3 mm × 3 mm and 150 × 150 mm, respectively. All the measurements were carried out at room temperature under ambient conditions.

*Time of Flight (TOF) Measurement*: The configuration of the sample is ITO/POSTF (2.1 μm)/Ag (20 nm)/Ag:Mg (130 nm), where ITO was cleaned by ultrasonication in ethanol–acetone (1:1) and deionized water. The POSTF film was fabricated by vacuum deposition in vacuum. The pressure was controlled to be lower than $1 \times 10^{-3}$ Pa. The deposition rate of POSTF was 0.3–0.4 nm $s^{-1}$. When finished, the sample was mounted in a vacuum chamber for the TOF measurement. A nitrogen pulsed laser (337.1 nm) radiated the sample from the ITO side to generate a thin sheet of excess carriers. The transient currents were recorded by a digital oscilloscope (500 MHz, 5GS $s^{-1}$). The transit time $\tau$ corresponds to the cross point of the asymptotes to the current curves with distinguishing slopes in the double logarithmic scale. The measurement was performed at room temperature.

*Syntheses of Materials*: STFBr was synthesized according to literature.[12] THF was purified by PURE SOLV (innovative technology) purification system. Other reactants or reagents were used as received. STFBr (1.95 g, 4 mmol) was dissolved in THF under argon in Schlenk tube. n-Butyl lithium (2.5 mL/2.4 M, 6 mmol) was added drop wise to the solution under –78 °C. After one hour's stirring, diphenylphosphine chloride (1.77 g, 8 mmol) was added via a syringe. Then the resulting mixture was allowed to warm up to room temperature overnight. To terminate the reaction, 5 mL water was added. And the organic solvent was removed by evaporation under reduced pressure. The resulting crude product was washed with water and submitted to flash column chromatography (petroleum ether/dichloromethane: 6/1, v/v as eluent), affording the diphenylphosphine substituted intermediate as a white solid. Then the diphenylphosphine derivatives were dissolved in DCM at room temperature. 3 mL $H_2O_2$ (30%) was added to the solution drop wise. After stirred at room temperature for 30 min, 50 mL water was added and organic layer was separated, dried, and evaporated under reduced pressure to afford the crude product. The crude products were further purified by recrystallization (using hexane and ethyl acetate as solvent) and vacuum sublimation. The final product is a white powder (2.04 g, 84.0%). $^1$H NMR ($CDCl_3$, 400 MHz) ($\delta$, ppm): 7.85–7.82 (m, 3H, Ar-H), 7.63–7.34 (m, 17H, Ar-H), 7.19 (*d*, *J* = 7.2 Hz, 2H, Ar-H), 6.91 (*t*, *J* = 7.2 Hz, 2H, Ar-H), 6.56 (*t*, *J* = 7.6 Hz, 2H, Ar-H), 6.38 (*d*, *J* = 7.6 Hz, 2H, Ar-H), 6.28 (*d*, *J* = 7.6 Hz, 2H, Ar-H). $^{13}$C NMR ($CDCl_3$, 100 MHz) ($\delta$, ppm): 156.56, 156.54, 156.24, 142.42, 142.41, 141.33, 140.67, 138.72, 133.22, 132.22, 132.11, 132.04, 131.81, 131.81, 131.13, 131.12, 131.04, 129.67, 129.63, 129.50, 128.50, 128.41, 128.41, 128.02, 127.43, 127.24, 126.34, 123.89, 120.61, 120.61, 120.11, 119.89, 114.80, 57.11. MS (EI): m/z calcd for: 607.21, found: 607.26. Anal. Calcd for C43H30NOP (%): C 84.99, H 4.98, N 2.30; found: C 85.13, H 4.87, N 2.21; IR (KBr) 3425, 3060, 1589, 1445, 1386, 1328, 1184, 1113, 746, 694, 543 $cm^{-1}$; MP: 292–293 °C.

## Supporting Information

Supporting Information is available from the Wiley Online Library or from the author.

## Acknowledgements

The authors thank Dr. Lian Duan from the Tsinghua University for conducting the time of flight measurement. The authors are grateful to the financial support from the Natural Science Foundation of China (Nos. 21202114, 21161160446, 61177016, and 61036009). This project is also funded by Collaborative Innovation Center (CIC) of Suzhou Nano Science and Technology, Soochow University, and by the Priority Academic Program Development of the Jiangsu Higher Education Institutions (PAPD).

Received: September 29, 2014
Revised: November 17, 2014
Published online:

[1] a) J. Kido, M. Kimura, K. Nagai, *Science* **1995**, *267*, 1332; b) M. A. Baldo, D. F. O'Brien, Y. You, A. Shoustikov, S. Sibley, M. E. Thompson, S. R. Forrest, *Nature* **1998**, *395*, 151; c) Y. Ma, H. Zhang, J. Shen, C. Che, *Syn. Met.* **1998**, *94*, 245; d) M. A. Baldo, S. Lamansky, P. E. Burrows, M. E. Thompson, S. R. Forrest, *Appl. Phys. Lett.* **1999**, *75*, 4; e) T.-F. Guo, S.-C. Chang, Y. Yang, R. C. Kwong, M. E. Thompson, *Org. Electron.* **2000**, *1*, 15; f) F. Steuber, J. Staudigel, M. Stossel, J. Simmerer, A. Winnacker, H. Spreitzer, F. Weissortel, J. Salbeck, *Adv. Mater.* **2000**, *12*, 130; g) C. Adachi, M. A. Baldo, S. R. Forrest, S. Lamansky, M. E. Thompson, R. C. Kwong, *Appl. Phys. Lett.* **2001**, *78*, 1622; h) J. M. Lupton, I. D. W. Samuel, M. J. Frampton, R. Beavington, P. L. Burn, *Adv. Funct. Mater.* **2001**, *11*, 287; i) X. Gong, J. C. Ostrowski, G. C. Bazan, D. Moses, A. J. Heeger, *Appl. Phys. Lett.* **2002**, *81*, 3711; j) X. Gong, M. R. Robinson, J. C. Ostrowski, D. Moses, G. C. Bazan, A. J. Heeger, *Adv. Mater.* **2002**, *14*, 581.

[2] a) M.-Y. Lai, C.-H. Chen, W.-S. Huang, T. Lin Jiann, T.-H. Ke, L.-Y. Chen, M.-H. Tsai, C.-C. Wu, *Angew. Chem. Int. Ed.* **2008**, *47*, 581; b) S.-J. Su, H. Sasabe, T. Takeda, J. Kido, *Chem. Mater.* **2008**, *20*, 1691; c) Y. Tao, Q. Wang, C. Yang, Q. Wang, Z. Zhang, T. Zou, J. Qin, D. Ma, *Angew. Chem. Int. Ed.* **2008**, *47*, 8104; d) Y. Tao, Q. Wang, C. Yang, K. Zhang, Q. Wang, T. Zou, J. Qin, D. Ma, *J. Mater. Chem.* **2008**, *18*, 4091; e) C.-H. Chien, F.-M. Hsu, C.-F. Shu, Y. Chi, *Org. Electron.* **2009**, *10*, 871; f) F.-M. Hsu, C.-H. Chien, P.-I. Shih, C.-F. Shu, *Chem. Mater.* **2009**, *21*, 1017; g) F.-M. Hsu, C.-H. Chien, C.-F. Shu, C.-H. Lai, C.-C. Hsieh, K.-W. Wang, P.-T. Chou, *Adv. Funct. Mater.* **2009**, *19*, 2834; h) S.-Y. Takizawa, V. A. Montes, P. Anzenbacher, *Chem. Mater.* **2009**, *21*, 2452; i) C. Han, Z. Zhang, H. Xu, J. Li, G. Xie, R. Chen, Y. Zhao, W. Huang, *Angew. Chem. Int. Ed.* **2012**, *51*, 10104; j) L.-S. Cui, Y. Liu, X.-D. Yuan, Q. Li, Z.-Q. Jiang, L.-S. Liao, *J. Mater. Chem. C* **2013**, *1*, 8177; k) E. Mondal, W.-Y. Hung, Y.-H. Chen, M.-H. Cheng, K.-T. Wong, *Chem. Eur. J.* **2013**, *19*, 10563; l) Z. Zhang, Z. Zhang, R. Chen, J. Jia, C. Han, C. Zheng, H. Xu, D. Yu, Y. Zhao, P. Yan, S. Liu, W. Huang, *Chem. Eur. J.* **2013**, *19*, 9549; m) C. Han, L. Zhu, F. Zhao, Z. Zhang, J. Wang, Z. Deng, H. Xu, J. Li, D. Ma, P. Yan, *Chem. Commun.* **2014**, *50*, 2670; n) Q. Li, L.-S. Cui, C. Zhong, Z.-Q. Jiang, L.-S. Liao, *Org. Lett.* **2014**, *16*, 1622; o) L. Wang, B. Pan, B. Wang, Y. Wang, P. Xu, J. Chen, D. Ma, *J. Mater. Chem. C* **2014**, *2*, 2466.

[3] a) A. Chaskar, H.-F. Chen, K.-T. Wong, *Adv. Mater.* **2011**, *23*, 3876; b) Y. Tao, C. Yang, J. Qin, *Chem. Soc. Rev.* **2011**, *40*, 2943; c) D. Kim, V. Coropceanu, J. L. Bredas, *J. Am. Chem. Soc.* **2011**, *133*, 17895; d) V. Subramanian, E. Varathan, D. Vijay, P. S. V. Kumar, *J. Mater. Chem. C* **2013**, *1*, 4261; e) K. S. Yook, J. Y. Lee, *Adv. Mater.* **2014**, *26*, 4218.

[4] a) S. J. Kim, Y. J. Kim, Y. H. Son, J. A. Hur, H. A. Um, J. Shin, T. W. Lee, M. J. Cho, J. K. Kim, S. Joo, J. H. Yang, G. S. Chae, K. Choi, J. Hyuk Kwon, D. Hoon Choi, *Chem. Commun.* **2013**, *49*, 6788; b) C. W. Lee, Y. Im, J.-A. Seo, J. Y. Lee, *Org. Electron.* **2013**, *14*, 2687; c) C. W. Lee, J. Y. Lee, *Chem. Commun.* **2013**, *49*, 1446; d) C. W. Lee, K. S. Yook, J. Y. Lee, *Org. Electron.* **2013**, *14*, 1009; e) M.-k. Leung, Y.-H. Hsieh, T.-Y. Kuo, P.-T. Chou, J.-H. Lee, T.-L. Chiu, H.-J. Chen, *Org. Lett.* **2013**, *15*, 4694; f) Y. H. Son, Y. J. Kim, M. J. Park, H.-Y. Oh, J. S. Park, J. H. Yang, M. C. Suh, J. H. Kwon, *J. Mater. Chem. C* **2013**, *1*, 5008; g) J. Li, L. Deng, G.-X. Wang, L.-Z. Wu, *J. Mater. Chem. C* **2013**, *1*, 8140; h) L.-S. Cui, Y. Liu, Q. Li, Z.-Q. Jiang, L.-S. Liao, *Org. Electron.* **2014**, *15*, 1368.

[5] a) J.-K. Bin, N.-S. Cho, J.-I. Hong, *Adv. Mater.* **2012**, *24*, 2911; b) C. W. Lee, J. Y. Lee, *Adv. Mater.* **2013**, *25*, 5450; c) C. W. Lee, J. Y. Lee, *Chem. Mater.* **2014**, *26*, 1616; d) H. Shin, S. Lee, K.-H. Kim, C.-K. Moon, S.-J. Yoo, J.-H. Lee, J.-J. Kim, *Adv. Mater.* **2014**, *26*, 4730.

[6] a) C. Fan, L. Zhu, B. Jiang, C. Zhong, D. Ma, J. Qin, C. Yang, *Org. Electron.* **2013**, *14*, 3163; b) S. Lee, S.-O. Kim, H. Shin, H.-J. Yun, K. Yang, S.-K. Kwon, J.-J. Kim, Y.-H. Kim, *J. Am. Chem. Soc.* **2013**, *135*, 14321; c) S. B. Meier, W. Sarfert, J. M. Junquera-Hernandez, M. Delgado, D. Tordera, E. Orti, H. J. Bolink, F. Kessler, R. Scopelliti, M. Gratzel, M. K. Nazeeruddin, E. Baranoff, *J. Mater. Chem. C* **2013**, *1*, 58; d) J. Zhuang, W. Li, W. Su, Y. Liu, Q. Shen, L. Liao, M. Zhou, *Org. Electron.* **2013**, *14*, 2596; e) N. Darmawan, C.-H. Yang, M. Mauro, R. Frohlich, L. De Cola, C.-H. Chang, Z.-J. Wu, C.-W. Tai, *J. Mater. Chem. C* **2014**, *2*, 2569; f) R. Srivastava, L. R. Joshi, *Phys. Chem. Chem. Phys.* **2014**, *16*, 17284; g) K. Udagawa, H. Sasabe, C. Cai, J. Kido, *Adv. Mater.* **2014**, *26*, 5062; h) K. E. Linton, A. L. Fisher, C. Pearson, M. A. Fox, L. Palsson, M. R. Bryce, Michael, C. Petty, *J. Mater. Chem.* **2012**, *22*, 11816; i) D. Thirion, M. Romain, J. R. Berthelot, C. Poriel, *J. Mater. Chem.* **2012**, *22*, 7149; j) L. Yao, S. Sun, S. Xue, S. Zhang, X. Wu, H. Zhang, Y. Pan, C. Gu, *J. Phys. Chem. C* **2013**, *117*, 14189.

[7] a) T. Spehr, R. Pudzich, T. Fuhrmann, J. Salbeck, *Org. Electron.* **2003**, *4*, 61; b) R. Pudzich, T. Fuhrmann-Lieker, J. Salbeck, *Adv. Polym. Sci.* **2006**, *199*, 83; c) J. Londenberg, T. P. I. Saragi, I. Suske, J. Salbeck, *Adv. Mater.* **2007**, *19*, 4049; d) T. P. I. Saragi, T. Spehr, A. Siebert, T. Fuhrmann-Lieker, J. Salbeck, *Chem. Rev.* **2007**, *107*, 1011; e) S. Tang, M. Liu, P. Lu, H. Xia, M. Li, Z. Xie, F. Shen, C. Gu, H. Wang, B. Yang, Y. Ma, *Adv. Funct. Mater.* **2007**, *17*, 2869; f) X. Xing, L. Xiao, L. Zheng, S. Hu, Z. Chen, B. Qu, Q. Gong, *J. Mater. Chem.* **2012**, *22*, 15136.

[8] K.-T. Wong, Y.-L. Liao, Y.-T. Lin, H.-C. Su, C.-c. Wu, *Org. Lett.* **2005**, *7*, 5131.

[9] W.-Y. Hung, T.-C. Tsai, S.-Y. Ku, L.-C. Chi, K.-T. Wong, *Phys. Chem. Chem. Phys.* **2008**, *10*, 5822.

[10] a) Y.-M. Jeon, I.-H. Lee, H.-S. Lee, M.-S. Gong, *Dyes Pigm.* **2011**, *89*, 29; b) J.-Y. Kim, C.-W. Lee, J. G. Jang, M.-S. Gong, *Dyes Pigm.* **2012**, *94*, 304; c) Z. Li, B. Jiao, Z. Wu, P. Liu, L. Ma, X. Lei, D. Wang, G. Zhou, H. Hu, X. Hou, *J. Mater. Chem. C* **2013**, *1*, 2183; d) S. Thiery, D. Tondelier, C. Declairieux, G. seo, B. Geffroy, o. Jeannin, J. Rault-Berthelot, R. Metivier, C. Poriel, *J. Mater. Chem. C* **2014**, *2*, 4156; e) S. Thiery, C. Declairieux, D. Tondelier, G. Seo, B. Geffroy, O. Jeannin, R. Métivier, J. Rault-Berthelot, C. Poriel, *Tetrahedron* **2014**, *70*, 6337; f) Y.-X. Zhang, L. Zhang, L.-S. Cui, C.-H. Gao, H. Chen, Q. Li, Z.-Q. Jiang, L.-S. Liao, *Org. Lett.* **2014**, *16*, 3748; g) C. Fan, Y. Chen, Z. Liu, Z. Jiang, C. Zhong, D. Ma, J. Qin, C. Yang, *J. Mater. Chem. C* **2013**, *1*, 463; h) J. Zhao, G. H. Xie, C. R. Yin, L. H. Xie, C. M. Han, R. F. Chen, H. Xu, M. D. Yi, Z. P. Deng, S. F. Chen, Y. Zhao, S. Y. Liu, W. Huang, *Chem. Mater.* **2011**, *23*, 5331.

[11] H. Chen, Z.-Q. Jiang, C.-H. Gao, M.-F. Xu, S.-C. Dong, L.-S. Cui, S.-J. Ji, L.-S. Liao, *Chem. Euro. J.* **2013**, *19*, 11791.

[12] Z. Jiang, Z. Liu, C. Yang, C. Zhong, J. Qin, G. Yu, Y. Liu, *Adv. Funct. Mater.* **2009**, *19*, 3987.

[13] a) S. O. Jeon, K. S. Yook, C. W. Joo, J. Y. Lee, *Appl. Phys. Lett.* **2009**, *94*, 013301; b) S. E. Jang, C. W. Joo, S. O. Jeon, K. S. Yook, J. Y. Lee, *Org. Electron.* **2010**, *11*, 1059.

[14] a) S. Gong, Y. Chen, C. Yang, C. Zhong, J. Qin, D. Ma, *Adv. Mater.* **2010**, *22*, 5370; b) S. Gong, Y. Chen, J. Luo, C. Yang, C. Zhong, J. Qin, D. Ma, *Adv. Funct. Mater.* **2011**, *21*, 1168; c) S. Gong, Y. Chen, X. Zhang, P. Cai, C. Zhong, D. Ma, J. Qin, C. Yang, *J. Mater. Chem.* **2011**, *21*, 11197; d) S. Gong, Q. Fu, Q. Wang, C. Yang, C. Zhong, J. Qin, D. Ma, *Adv. Mater.* **2011**, *23*, 4956; e) S. Gong, N. Sun, J. Luo, C. Zhong, D. Ma, J. Qin, C. Yang, *Adv. Funct. Mater.* **2014**, *24*, 5710.

[15] a) H. E. Simmons, T. Fukunaga, *J. Am. Chem. Soc.* **1967**, *89*, 5208; b) P. Maslak, A. Chopra, C. R. Moylan, R. Wortmann, S. Lebus, A. L. Rheingold, G. P. A. Yap, *J. Am. Chem. Soc.* **1996**, *118*, 1471.